HHS Public Access

Author manuscript

Nature. Author manuscript; available in PMC 2013 May 22.

Published in final edited form as:

Nature. 2012 November 22; 491(7425): 613–617. doi:10.1038/nature11546.

Accelerated Disassembly of IgE:Receptor Complexes by a Disruptive Macromolecular Inhibitor

Beomkyu Kim[1,†], **Alexander Eggel**[2,†], **Svetlana S. Tarchevskaya**[1], **Monique Vogel**[2], **Heino Prinz**[3], and **Theodore S. Jardetzky**[1,*]

[1]Department of Structural Biology, Stanford University School of Medicine, Stanford, California, 94305, USA [2]University Institute of Immunology, University of Bern, Inselspital, Sahlihaus 2, CH-3010 Bern, Switzerland [3]Max-Planck-Institut fur Molekulare Physiologie, Otto-Hahn-Str. 11,44227 Dortmund, Germany

Abstract

IgE antibodies bind the high affinity IgE Fc receptor (FcεRI), found primarily on mast cells and basophils, and trigger inflammatory cascades of the allergic response[1,2]. Inhibitors of IgE:FcεRI binding have been identified and an anti-IgE therapeutic antibody (omalizumab) is used to treat severe allergic asthma[3,4]. However, preformed IgE:FcεRI complexes that prime cells prior to allergen exposure dissociate extremely slowly[5] and cannot be disrupted by strictly competitive inhibitors. IgE-Fc conformational flexibility indicated that inhibition could be mediated by allosteric or other non-classical mechanisms[6–8]. Here we demonstrate that an engineered protein inhibitor, DARPin E2_79[9–11], acts through a non-classical inhibition mechanism, not only blocking IgE:FcεRI interactions, but actively stimulating the dissociation of preformed ligand-receptor complexes. The structure of the E2_79:IgE-Fc_{3-4} complex predicts the presence of two non-equivalent E2_79 sites in the asymmetric IgE:FcεRI complex, with Site 1 distant from the receptor and Site 2 exhibiting partial steric overlap. While the structure is suggestive of an allosteric inhibition mechanism, mutational studies and quantitative kinetic modeling indicate that E2_79 acts through a facilitated dissociation mechanism at Site 2 alone. These results demonstrate that high affinity IgE:FcεRI complexes can be actively dissociated to block the allergic response and suggest that protein:protein complexes may be more generally amenable to active disruption by macromolecular inhibitors.

*Corresponding author: Theodore S. Jardetzky, Gilbert Biological Sciences Building, 371 Serra Mall, Room 228, Stanford, CA 94305, (p) (650) 498-4179, (f) (650) 723-4943, (e) tjardetz@stanford.edu.

†these authors contributed equally.

AUTHOR CONTRIBUTIONS.

B.K., A.E., S.T. and T.S.J designed and performed experiments and analyzed data. B.K., S.T., A.E., M.V and T.S.J. contributed reagents, discussed/commented on results and edited the manuscript. B.K., A.E., and T.S.J. wrote the manuscript and supplementary information, and prepared the figures.

The structure factors and model for the E2_79:C335 IgE complex have been deposited in the RSCB under PDB ID code 4GRG.

The authors declare no competing financial interests.

The IgE antibody Fc, comprised of three domains (Cε2-Cε3-Cε4), binds the α-chain of FcεRI (FcεRIα) with subnanomolar affinity (<1 nM)[1,2]. The IgE-Fc Cε3 domains contact receptor directly and can adopt multiple conformational states, ranging from closed to open forms[6–8,12], which could impact FcεRI binding and potential receptor complex dynamics. In an effort to characterize different IgE ligands and mechanisms of FcεRI inhibition, we developed a fluorescence-binding assay that distinguishes IgE ligands using a site-specific reporter fluorophore. A double mutant (C328A/K367C) of the IgE-Fc Cε3-Cε4 protein (IgE-Fc_{3-4}) was labeled with Alexa Fluor 488 at residue 367 (referred to as AF488-Fc), which is adjacent to the FcεRIα binding site (Supplementary Figure 1). AF488-Fc exhibited systematic fluorescence quenching with increasing concentrations of FcεRIα (Figure 1a), yielding a Kd of ~22 nM (Supplementary Table 1) consistent with the lower affinity of the C328A mutation[13]. FcεRIα-directed inhibitors, such as unlabeled IgE-Fc_{3-4} and anti-FcεRIα antibody (mAb 15.1)[14,15] reversed receptor-induced fluorescence quenching (Figure 1b,c and Supplementary Table 1),

IgE-directed inhibitors, including the anti-IgE antibody omalizumab (Xolair)[3,4], a 34-mer DNA aptamer (D17.4)[16,17], and DARPin E2_79[9–11], yielded three inhibition profiles. Xolair induced fluorescence quenching comparable to FcεRIα (Figure 1d and Supplementary Table 1), consistent with its binding an epitope overlapping the FcεRIα site[18,19]. E2_79 restored the receptor-quenched fluorescence signal (Figure 1e and Supplementary Table 1), similar to FcεRIα-binding inhibitors (Figure 1b,c). D17.4 did not quench or compete with FcεRIα, but in an indirect competitive binding experiment with AF488-Fc, FcεRIα and unlabeled wt IgE-Fc_{3-4}, D17.4 induced systematic fluorescence quenching (Figure 1f and Supplementary Table 1), consistent with D17.4 binding to wt IgE-Fc_{3-4} but not AF488-Fc. These data indicated that D17.4 and Xolair act as direct competitive inhibitors, but E2_79 was a candidate allosteric inhibitor.

We determined the 4.3Å crystal structure of E2_79 bound to IgE-Fc_{3-4} (Supplementary Table 2), using a cysteine mutant (C335) that locks the Fc into a closed conformational state (manuscript submitted). E2_79 binds the IgE Cε3 domain and does not directly engage residues involved in FcεRIα binding (Figure 2a,b). E2_79 interactions extend throughout the Cε3 domain, including the Cε3-Cε4 domain linker and encroaching on FcεRIα-binding loops (Figure 2a,c).

To examine the structural basis for E2_79 inhibition, we superimposed the E2_79 structure onto the IgE-Fc:FcεRIα complex using the IgE Cε3 domains. The IgE-Fc:FcεRIα complex is asymmetric, defining two distinct E2_79 sites (Figure 2b). In the complex, Site 1 is entirely exposed, with E2_79 and FcεRIα separated by ~20 Å and no steric overlap (Figure 2b), indicating the potential for simultaneous E2_79 and FcεRIα binding. For Site 2, three E2_79 and five FcεRIα residues make contacts <3.5Å (Supplementary Table 3), causing partial steric overlap.

We generated three E2_79 double mutants (E20A-R23A, Y45A-W46A, and E126A-D127A) to probe the inhibition mechanism (Figure 2c). E20 and R23 are located adjacent to the Cε3-Cε4 domain linker and could affect the Cε3 domain conformational state, allosterically inhibiting FcεRIα. Y45 and W46 are in the hydrophobic interface with the

IgE-Fc, and are likely important for binding affinity. E126 and D127 account for the majority of predicted steric conflicts with FcεRI at Site 2 (Supplementary Table 3) and could potentially interact with the FcεRI FG binding loop containing R427, contributing to the inhibition. The E20A-R23A and E126A-D127A mutants exhibited similar binding affinity to IgE-Fc as "wt" E2_79 (Figure 3a,b), while the Y45A-W46A mutant showed significantly reduced binding affinity (Figure 3c). The inhibition activities of the E20A-R23A and E126A-D127A mutants remained similar to the wt E2_79 (Figure 3d,e), suggestive of a non-allosteric model. The Y45A-W46A mutant exhibited no inhibition (Figure 3f), as expected from its lack of binding (Figure 3c). The mutants validated the crystal structure, and indicated that E2_79 inhibition is not due to Cε3-Cε4 linker or FcεRI binding loop interactions.

To investigate binding of E2_79 to the IgE:FcεRIα complex, we conducted Biacore experiments that revealed a dramatic acceleration of complex disassembly. FcεRIα was coupled to the chip, then loaded with either full length IgE (Sus11) or IgE-Fc_{3-4} proteins (Supplementary Figure 2). The anti-IgE antibody Le27 recognizes a non-inhibitory epitope in the IgE Cε4 domain and binding to the preformed IgE:FcεRIα complexes was readily observed (Supplementary Figure 2a,e). In contrast, E2_79, but not controls, stimulated rapid dissociation of both Sus11 and IgE-Fc_{3-4} complexes (Supplementary Figure 2b–d,f–h).

E2_79 and FcεRIα binding to IgE are linked by a 6 state coupled binding reaction scheme (Figure 4a,b), in which two E2_79 molecules and one FcεRIα protein can potentially assemble into a quaternary complex with IgE. We considered three potential mechanisms to explain the accelerated complex dissociation: (1) a classic competitive inhibition mechanism operating solely through steric conflicts at Site 2; (2) an allosteric mechanism operating through both Site 1 and Site 2; (3) a facilitated dissociation mechanism, in which E2_79 binding to IgE:FcεRIα complexes only at Site 2 stimulates complex dissociation. Model 3 represents a competitor-induced dissociation mechanism[20], in which a subset of ligand attachment points that become exposed during partial complex dissociation can be engaged by an exogeneously added competitor, thereby accelerating the intrinsic dissociation rate. This has been named "facilitated dissociation"[21]. To quantitatively discriminate between the three inhibition mechanisms, we developed the complete reaction schemes as COPASI biochemical network models[22], allowing the simulation of the time-dependent evolution of the reaction pathways and intermediates, as well as global curve fitting and parameter estimation with the SPR data.

The classic competitive inhibition mechanism is not consistent with the SPR data, but predicts high affinity binding of E2_79 to Site 1 and no acceleration of IgE release from the chip surface (Supplementary Figure 3a,b). Simulations for this model are similar to the experimental observations with the Le27 antibody (Supplementary Figure 2a,e). In this model, E2_79 competition is only mediated by Site 2, where steric hindrance prevents E2_79 binding to IgE:FcεRIα complexes. Relaxation to a new equilibrium occurs with the unaccelerated, slow dissociation rate of the complex.

For the allosteric model, we posited that both Site 1 and Site 2 would contribute to FcεRIα inhibition and the acceleration of complex dissociation. In this model, E2_79 binding to

Sites 1 and 2 in the IgE:FcεRIα complex should both exhibit reduced affinity associated with the allosteric coupling. Similarly, both Site 1 and Site 2 binding by E2_79 would induce reduced affinity and increased dissociation rates for FcεRIα (Figure 4a). Due to this allosteric coupling, IgE:FcεRIα complexes should not have any high affinity binding sites for E2_79.

For the facilitated dissociation model, we posited that E2_79 binding to Site 1 is not affected by FcεRIα binding, consistent with the predicted >20Å distance between these proteins (Figure 2b,4b). There is also correspondingly no change in FcεRIα binding affinity associated with E2_79 binding to Site 1. The rate constants for both of these binding steps were initially set to the experimentally determined rate constants for E2_79 and FcεRIα binding in the absence of the other ligand. In this model, only the binding affinity of E2_79 at Site 2 is reduced by FcεRIα, through this non-classical competition mechanism. Similarly, there must be a corresponding reduction in FcεRIα binding affinity in the quaternary E2_79:IgE:FcεRIα:E2_79 complex. Importantly, in this model, Site 1 retains native high affinity for E2_79 in the IgE:FcεRIα complex, while only Site 2 exhibits reduced E2_79 affinity and the ability to accelerate FcεRIα dissociation. This distinguishes it from the allosteric model, which lacks any high affinity E2_79 sites in the complex.

The initial 120 seconds of SPR data for IgE-Fc_{3-4} (Supplementary Figure 2h), covering E2_79 concentrations from 100 nM – 10 μM, were simultaneously fit using the allosteric and facilitated dissociation COPASI models. Curve fitting (Figure 4c–f) demonstrates that only the facilitated dissociation mechanism captures the biphasic behavior of the SPR traces accurately. The SPR data exhibit an ~50 RU, E2_79 concentration-dependent association phase within the first 10–20 seconds that cannot be modeled by the full allosteric mechanism (Figure 4c,d). While both models fit the later concentration dependent dissociation rates for the IgE:FcεRIα complexes, the initial 10–20 seconds demonstrate an association that corresponds to the presence of the high affinity binding of E2_79 to the exposed Site 1 within the IgE:FcεRIα complex. Given the robustness of the fitting, we allowed Site 1 kinetic constants in the facilitated dissociation model to vary from experimental values for both E2_79 and FcεRIα (Supplementary Table 4). This provided slightly improved curve fitting, while the fitted E2_79 Site 1 kinetic constants remained close to those determined for the independently binding ligand, further validating this model over an allosteric one.

Non-classical or allosteric inhibitors have the general potential to not only block receptor-ligand binding, but to also engage and actively dissociate preformed receptor complexes. For the IgE:FcεRIα interaction, the activated release of receptor-bound antibody on the surface of effector cells might prove beneficial in treating acute allergic reactions. Here we demonstrated that the E2_79 DARPin is a disruptive inhibitor that binds to IgE:FcεRIα complexes, dramatically accelerating their dissociation orders of magnitude over the unaccelerated intrinsic rate.

It has been proposed that facilitated dissociation occurs through competition for subsite attachment points within a ligand binding site, which become partially exposed prior to full ligand dissociation[20,21]. In principle, competitor-induced acceleration of ligand dissociation

can be explained by multiple mechanisms, such as allosteric or facilitated dissociation mechanisms considered here, but few observations have been fully examined by both structural and kinetic methods. Small molecule inhibitors of TNF have been shown to accelerate the dissociation of TNF trimers[23,24], potentially intercalating into the trimeric interface. It has been suggested, and it is likely commonly assumed, that larger macromolecular inhibitors depend on complete dissociation of protein complexes and would be unlikely to engage partially dissociated intermediates, potentially providing a "kinetic advantage" to small molecule protein interaction inhibitors[24]. However, the E2_79 induced dissociation of IgE:FcεRIα complexes suggests that macromolecular therapeutics may have untapped potential as disruptive inhibitors. Antibody-induced complex dissociation has been observed, but specific mechanisms and requirements for such accelerated dissociation have not been fully investigated[25–27]. Facilitated dissociation may also play an unappreciated role in naturally evolved macromolecular complex disassembly processes.

METHODS

Mutagenesis

IgE-Fc_{3-4} mutants for the fluorescence assay (C328A/G335C, C328A/K367C, T369C, and R427C) were generated by site-directed mutagenesis (QuickChange Kit: Stratagene) or made commercially (Mutagenix) and confirmed by DNA sequencing. We refer to the resulting double C328A/G335C and C328A/K367C IgE-Fc_{3-4} mutant proteins as C335 IgE-Fc_{3-4} and C367 IgE-Fc_{3-4}, respectively. E2_79 mutations (E20A-R23A, Y45A-W46A, W89A, and E126A-D127A) were introduced into the original E2_79 gene[9–11]. The E2_79 mutants for the binding assays were generated by site-directed mutagenesis (QuickChange Kit: Stratagene) and confirmed by DNA sequencing.

Expression and purification of proteins

Expression and purification of the soluble FcεRI α-chain ectodomain was carried out as previously described[12,28]. Omalizumab (Xolair) was purchased from Novartis. MAb15.1 (anti-FcεRIα) was a kind gift of the Kinet laboratory. Selection and characterization of the DARPin E2_79 has been reported elsewhere[10]. Expression and purification of the E2_79 mutants were carried out as previously described[10]. The IgE-Fc_{3-4} cysteine mutants were expressed in insect cells. The wt IgE-Fc_{3-4}, C367 and C335 IgE-Fc_{3-4} proteins were also cloned into pENTR1A (Invitrogen) using a Kpn I-Xho I fragment and transferred into the BaculoDirect C-term Linear DNA by using LR Clonase II Enzyme Mix (Invitrogen). Recombinant baculoviruses expressing wt and C367 IgE-Fc_{3-4} proteins were generated using BaculoDirect C-term Transfection Kit (Invitrogen). Recombinant virus was selected and amplified following standard protocols. The wt and C367 IgE-Fc_{3-4} proteins include 3 non-native residues (ADP) generated by the construct at the N-terminus and 48 non-native residues including a V5 epitope and a histidine affinity tag (His-tag) at the C-terminus. For protein production, Hi5 insect cells were grown to a density of 1.3~1.5 million cells/ml and infected with the baculovirus stocks of recombinant the wt and C367 IgE-Fc_{3-4} proteins. Cell supernatants were harvested 2.5 ~ 3 days post-infection and filtered through a Durapore 0.45 μm filter (Millipore). The supernatants were incubated with Ni-NTA agarose (Invitrogen) at room temperature for 3h, and then loaded into a column. The column was

rinsed with 4–5 column volumes of the washing buffer (50 mM Tris [pH 8], 50 mM Imidazole, and 300 mM NaCl), and IgE-Fc_{3-4} was eluted directly with the elution buffer (50 mM Tris [pH 8], 200 mM Imidazole, and 300 mM NaCl). The samples were dialyzed and concentrated in buffer (50 mM Tris [pH 8] and 50 mM NaCl) using an Amicon ultrafiltration device (Millipore) to a protein concentration of 1 mg/ml. Proteins were quantified using a Nanodrop spectrophotometer using an extinction coefficient of e=1.32 $cm^{-1}(mg/ml)^{-1}$ at 280 nm[8]. To remove the C-terminal tag residues, purified IgE-Fc_{3-4} was concentrated to 2~3 mg/ml and treated with 5–10 U recombinant enterokinase (Invitrogen) per 1 mg protein at room temperature overnight. The enzyme was removed using Ekapture agarose (Novagen).

Dye labeling of AF488-Fc

Purified C367 IgE-Fc_{3-4} was incubated with three molar equivalents of TCEP (Tris(2-Carboxyethyl)phosphine) at room temperature for 1h. Following TCEP treatment, the presence of free thiol groups in the C367 was confirmed using a Thiol and Sulfide Quantitation Kit (Molecular Probes). Cysteine-reactive Alexa Fluor 488 (maleimide derivative) was purchased from Invitrogen/Molecular Probes and dissolved in DMSO (Dimethyl Sulfoxide) at a concentration of 1 mg/ml. The C367 IgE-Fc_{3-4} was incubated with 5 molar equivalents of Alexa Fluor 488, at 4 C overnight. Unreacted dye was removed by gel filtration on a Superdex 200 column (GE Healthcare) equilibrated in buffer (50 mM Tris [pH 8] and 50 mM NaCl).

Fluorescence measurements

Fluorescence experiments were performed using a Synergy 4 multi-mode plate reader (BioTek) in black 96-well Costar fluorescence plates (Corning) in assay buffer (50 mM Tris [pH 8], 50 mM NaCl, 0.1 % (v/v) Tween-20, and 100 nM BSA (bovine serum albumin)) at room temperature. Fluorescence was measured using an excitation wavelength of 488 nm and emission was monitored at 520 nm. All samples were incubated at room temperature for at least 10 min before measurement. All measurements were recorded in duplicate. Data obtained were analyzed and plotted using KaleidaGraph (Synergy). Binding constants (Kd) of FcεRIα and Xolair, and half maximal effective concentrations (EC50) of wt IgE-Fc_{3-4}, mAb15.1, D17.4 and E2_79 were obtained by fitting the experimental data to a standard Michaelis-Menten model. The oligonucleotide ligand (D17.4)[17] was synthesized by the PAN Facility (Stanford University School of Medicine).

To monitor fluorescence quenching each well in a black plate contained 1 μg/ml AF488-Fc and increasing concentrations of FcεRIα (0–200 nM) or Xolair (0–250 nM) in the fluorescence buffer in a total volume of 100 μl. For direct competition assays, each well in a black 96-well plate contained 1 μg/ml AF488-Fc, 50 nM FcεRIα, and one of the following competitors: unlabeled wt IgE- Fc_{3-4} (0–200 nM), mAb15.1 (0–100 nM), and E2_79 (0–200 nM). FcεRIα and competitors (except for mAb15.1) were mixed together, and AF488-Fc was added last. For competition assays with mAb 15.1, AF488-Fc and mAb15.1 were mixed together, and FcεRIα was added last.

For the double competition assay with D17.4, each well in a black 96-well plate contained 1 μg/ml AF488-Fc, 50 nM unlabeled wt IgE-Fc_{3-4}, 50 nM FcεRIα, and increasing concentrations of D17.4 (0–200 nM) in the fluorescence buffer in a final volume of 100 μl. D17.4 ligand was annealed at 70°C and cooled prior to use. The AF488-Fc and unlabeled wt IgE-Fc_{3-4} were mixed together, and then 50 nM FcεRIα and D17.4 were added last together.

Biacore binding assays

SPR assays were conducted with a BIAcore X100 machine and evaluated with BIAevaluation Software, as well as the specific COPASI models described below. Recombinant FcεRIα, corresponding to a previously described N- and C-terminal fusion of FcεRIα with human serum albumin[10], was coupled to the CM5 chip surface. The surface of both flow cells on the CM5 chip were activated with EDC + NHS (both flow cells). Target was injected only in flow cell 2 at 10 μg/ml until the target response of 2500 RU or 700 RU was reached. The surfaces of both flow cells were deactivated with Ethanolamine. In all experiments the response (non-specific binding) in flow cell 1 is subtracted from the signal of flow cell 2. 10 nM IgE was injected for 2 min. The maximal response (t=360 s) is set to 0. The off-rate of IgE (buffer flow) was observed for 3 min. Since the interaction of IgE with FceRIa is very high (~1 × 10–10 M) almost no off-rate is observable in this short time. Thus the baseline is very stable (almost horizontal), providing an ideal condition to test the binding of a third molecule to the FcεRIα:IgE complex. Different concentrations of anti-IgE molecules were tested. For each measurement new IgE was added to the immobilized FcεRIα since the chip surface was regenerated (stripped) after each run (each concentration of every binder) with 50 mM NaOH. The anti-IgE molecules were injected for 2 min. Dissociation was again observed for 3 min. E2_79 as well as control IgG were tested with FcεRIα alone (without IgE) and no binding was observed.

Protein crystallization

The C335 IgE-Fc_{3-4}/E2_79 protein was concentrated to ~10 mg/ml in the buffer (50 mM Tris [pH 8] and 50 mM NaCl) using Vivaspin 500 (Sartorius) concentrators, and the final concentration was confirmed using a Nanodrop spectrophotometer (Nanodrop Technologies) with a theoretical absorbance of 0.1% of 1.108 at 280 nm. Initial crystallization conditions were found by sitting drop vapor diffusion at room temperature using Qiagen JCSG Core Suite screens (Qiagen), and optimized by hanging drop vapor diffusion methods. The best crystals of C335 IgE-Fc_{3-4}/E2_79 were ontained in 1~3 days by mixing 0.5 μl of protein mixed with 0.5 μl of reservoir solution (0.1 M Phosphate-citrate [pH 4.2], 5% (w/v) PEG-3000, 25% (v/v) 1,2-propanediol, 10% (v/v) glycerol; final pH of ~5) and incubating over 600 μl of reservoir solution. The crystals were transferred into harvest buffer (0.1 M phosphate-citrate [pH 4.2], 8% (w/v) PEG-3000, 25% (v/v) 1,2-propanediol, 10% (v/v) glycerol), and then flash-cooled in liquid nitrogen.

X-ray data collection, molecular replacement, and refinement

Data was collected on beamline 8.3.1 at the Advanced Light Source. All data were indexed, integrated, and scaled using the programs Denzo and Scalepack in the HKL2000 suite[29]. The C335:E2_79 crystal grew in space group $P3_2$, with unit cell dimensions a = 71.3 Å, b =

71.3 Å, *c* = 178.5 Å, and γ= 120°. The structure was solved by molecular replacement with Phaser[30], using high-resolution crystal structure of the wt IgE-Fc_{3-4} and a homologous DARPin (PDB ID Code 3HG0) as the starting models. Iterative rounds of coordinate and B-factor refinement were done with Refmac, interspersed with manual model building in Coot[31]. The final model was refined to ~4.3 Å with statistics collected in Supplementary Table 2. The geometry of the complex model was assessed using MolProbity[32] and PROCHECK[33].

ELISA Binding assays with E2_79 mutants

100 μl of purified IgE-Fc_{3-4} was incubated in microtiter plates overnight at 4 degrees at a concentration of 1 μg/ml in 0.05 M sodium carbonate buffer. Plates were rinsed and blocked by the same procedures used in the FcεRI binding assay. E2_79 mutants with His-tag for E20A-R23A, Y45A-W46A, and E126A-D127A (ranging from 0 nM to 200 nM or 400 nM) were added in duplicate to wells coated with the purified IgE-Fc_{3-4}. The binding of E2_79 with His-tag to plate-bound IgE-Fc_{3-4} was monitored using anti-His tag antibody (Novagen, 70796-3) as a primary antibody and anti-mouse IgG HRP conjugated antibody (R&D system, HAF007) as the secondary antibody. The anti-His tag antibody in a 1:1000 dilution was incubated after washing for 1 hour at room temperature, and then, the anti-mouse IgG HRP conjugated antibody was incubated after washing for 1 hour at room temperature. Plates were washed and developed using TMB single solution (Invitrogen, 00-2023). Microplates were read using a Synergy 4 multi-mode plate reader (BioTek) at 650 nm.

COPASI modeling

The COPASI software package for quantitative modeling of biochemical networks[22] was used to build the full reaction schemes presented in Figure 4 and Supplementary Figure 3. The model consists of 8 species and 7 reactions within a single compartment. Global quantities were defined, corresponding to on/off rates for the reaction steps associated with each mechanism, a consolidated "Biacore Output" (RU_{calc}) corresponding to reaction intermediates bound to the chip surface, a fractional mass weighting constant (F_{ME}) to account for E2_79 chip-bound species and overall scaling (k_{ov}) and baseline constants (C_0) for fitting the experimental SPR data. The Biacore Output (RU_{calc}) represents a combination of the three receptor-bound species affecting the SPR measurements and was defined mathematically as:

$$\mathrm{RU_{calc}}=k_{\mathrm{ov}}{}^{*}([\mathrm{IgE{:}Fc\varepsilon RI}]_t+(1+F_{\mathrm{ME}})^{*}[\mathrm{E2\_\ 79{:}IgE{:}Fc\varepsilon RI}]_t+(1+2^{*}F_{\mathrm{ME}})^{*}[E2\_\ 79{:}\mathrm{IgE{:}Fc\varepsilon RI}{:}E2\_\ 79]_t)+C_0$$

where $[IgE:Fc\varepsilon RI]_t$, $[E2\_79:IgE:Fc\varepsilon RI]_t$ and $[E2\_79:IgE:Fc\varepsilon RI:E2\_79]_t$ represent the time-dependent evolution of these reaction species as numerically simulated by COPASI, using the specific model restrictions. Biacore data were extracted using the BiaEvaluation software and imported directly into COPASI for parameter estimation. Each kinetic time course includes 120 data points (seconds), corresponding to a total of 840 data points for the simultaneous fitting of the model parameters. Data fitting was carried out with all available convergence methods, with best results obtained with simulated annealing, particle swarm, Hook & Jeeves, and Levenberg-Marquardt algorithms. The stable convergence of these

multiple methods to similar end points was taken as an indicator of the robustness of the fitting and the convergence to a common, global minimum. Experimentally determined rate constants for E2_79 and FcεRIα were determined in independent Biacore experiments and allowed to vary by 2–3-fold during the data fitting. E2_79 concentrations used experimentally were also allowed to vary up to 25% and F_{ME} was allowed to vary from 0–1. For the allosteric model, kinetic rate constants for Site 1 and Site 2 E2_79:IgE:FcεRIα complexes were set to be equivalent. These 4 parameters were allowed to vary freely, along with k_{ov} and C_0 yielding a total of 6 freely varying parameters. For the initial fitting of the facilitated dissociation model, kinetic rate constants for Site 1 were restricted to experimentally determined values for E2_79 binding in the absence of FcεRIα, and only the four kinetic constants associated with Site 2 E2_79:IgE:FcεRIα:E2_79 complexes were allowed to vary freely, also yielding a total of 6 freely varying parameters. For the full fitting of the facilitated dissociation model, kinetic rate constants for both Site 1 and Site 2 complexes were allowed to vary widely, yielding a total of 10 highly varying parameters.

Supplementary Material

Refer to Web version on PubMed Central for supplementary material.

Acknowledgments

We thank past and present members of the Jardetzky Laboratory. This research was supported in part by an NIH research grant to TSJ (AI-18939) and an American Asthma Foundation Senior Investigator Award as well as the Swiss National Science Foundation grant number 310030_127350. We also thank Prof. C. A. Dahinden and Prof. B. M. Stadler and members of their groups for valuable discussions. Further, we thank Molecular Partners AG, especially Patrick Amstutz, Michael T. Stumpp, Patrik Forrer and Daniel Steiner, for placing DARPin libraries at our disposal and providing scientific support.

References

1. Kraft S, Kinet JP. New developments in FcepsilonRI regulation, function and inhibition. Nat Rev Immunol. 2007; 7:365–78. [PubMed: 17438574]
2. Gould HJ, Sutton BJ. IgE in allergy and asthma today. Nat Rev Immunol. 2008; 8:205–17. [PubMed: 18301424]
3. D'Amato G, Bucchioni E, Oldani V, Canonica W. Treating Moderate-to-Severe Allergic Asthma with a Recombinant Humanized Anti-IgE Monoclonal Antibody (Omalizumab). Treat Respir Med. 2006; 5:393–8. [PubMed: 17154668]
4. Chang TW. The pharmacological basis of anti-IgE therapy. Nat Biotechnol. 2000; 18:157–162. [PubMed: 10657120]
5. Holdom MD, et al. Conformational changes in IgE contribute to its uniquely slow dissociation rate from receptor FcvarepsilonRI. Nat Struct Mol Biol. 2011; 18:571–6. [PubMed: 21516097]
6. Dhaliwal B, et al. Crystal structure of IgE bound to its B-cell receptor CD23 reveals a mechanism of reciprocal allosteric inhibition with high affinity receptor Fc{varepsilon}RI. Proc Natl Acad Sci U S A. 2012
7. Wurzburg BA, Jardetzky TS. Conformational flexibility in immunoglobulin E-Fc 3–4 revealed in multiple crystal forms. J Mol Biol. 2009; 393:176–90. [PubMed: 19682998]
8. Wurzburg BA, Garman SC, Jardetzky TS. Structure of the human IgE-Fc Ce3-Ce4 reveals conformational flexibility in the antibody effector domains. Immunity. 2000; 13:375–385. [PubMed: 11021535]
9. Eggel A, Baumann MJ, Amstutz P, Stadler BM, Vogel M. DARPins as bispecific receptor antagonists analyzed for immunoglobulin E receptor blockage. J Mol Biol. 2009; 393:598–607. [PubMed: 19683003]

10. Baumann MJ, Eggel A, Amstutz P, Stadler BM, Vogel M. DARPins against a functional IgE epitope. Immunol Lett. 2010; 133:78–84. [PubMed: 20673836]
11. Eggel A, et al. Inhibition of ongoing allergic reactions using a novel anti-IgE DARPin-Fc fusion protein. Allergy. 2011; 66:961–8. [PubMed: 21272035]
12. Garman SC, Wurzburg BA, Tarchevskaya SS, Kinet JP, Jardetzky TS. Structure of the Fc fragment of human IgE bound to its high-affinity receptor Fc epsilonRI alpha. Nature. 2000; 406:259–66. [PubMed: 10917520]
13. Basu M, et al. Purification and characterization of human recombinant IgE-Fc fragments that bind to the human high affinity IgE receptor. J Biol Chem. 1993; 268:13118–27. [PubMed: 7685756]
14. Wang B, et al. Epidermal Langerhans cells from normal human skin bind monomeric IgE via Fc epsilon RI. J Exp Med. 1992; 175:1353–65. [PubMed: 1533243]
15. Mirkina I, Schweighoffer T, Kricek F. Inhibition of human cord blood-derived mast cell responses by anti-Fc epsilon RI mAb 15/1 versus anti-IgE Omalizumab. Immunol Lett. 2007; 109:120–8. [PubMed: 17368811]
16. Mendonsa SD, Bowser MT. In vitro selection of high-affinity DNA ligands for human IgE using capillary electrophoresis. Anal Chem. 2004; 76:5387–92. [PubMed: 15362896]
17. Wiegand TW, et al. High-affinity oligonucleotide ligands to human IgE inhibit binding to Fc epsilon receptor I. J Immunol. 1996; 157:221–30. [PubMed: 8683119]
18. Zheng L, et al. Fine epitope mapping of humanized anti-IgE monoclonal antibody omalizumab. Biochem Biophys Res Commun. 2008; 375:619–22. [PubMed: 18725193]
19. Wright JD, Lim C. Prediction of an anti-IgE binding site on IgE. Protein Eng. 1998; 11:421–7. [PubMed: 9725620]
20. Prinz H, Striessnig J. Ligand-induced accelerated dissociation of (+)-cis-diltiazem from L-type Ca2+ channels is simply explained by competition for individual attachment points. J Biol Chem. 1993; 268:18580–5. [PubMed: 8395510]
21. Gutfreund, H. Kinetics for the Life Sciences. Receptors, Transmitters and Catalysts. Cambridge University Press; Cambridge, UK: 1995.
22. Hoops S, et al. COPASI--a COmplex PAthway SImulator. Bioinformatics. 2006; 22:3067–74. [PubMed: 17032683]
23. He MM, et al. Small-molecule inhibition of TNF-alpha. Science. 2005; 310:1022–5. [PubMed: 16284179]
24. Wells JA, McClendon CL. Reaching for high-hanging fruit in drug discovery at protein-protein interfaces. Nature. 2007; 450:1001–9. [PubMed: 18075579]
25. Wang CC, et al. Negative and positive site-site interactions, and their modulation by pH, insulin analogs, and monoclonal antibodies, are preserved in the purified insulin receptor. Proc Natl Acad Sci U S A. 1988; 85:8400–4. [PubMed: 3054887]
26. Lowenthal JW, et al. High and low affinity IL 2 receptors: analysis by IL 2 dissociation rate and reactivity with monoclonal anti-receptor antibody PC61. J Immunol. 1985; 135:3988–94. [PubMed: 3934270]
27. Boulain JC, Menez A. Neurotoxin-specific immunoglobulins accelerate dissociation of the neurotoxin-acetylcholine receptor complex. Science. 1982; 217:732–3. [PubMed: 7100919]
28. Garman SC, Kinet JP, Jardetzky TS. Crystal structure of the human high-affinity IgE receptor. Cell. 1998; 95:951–61. [PubMed: 9875849]
29. Otwinowski, Z.; Minor, W. Processing of X-ray Diffraction Data Collected in Oscillation Mode. In: Carter, CW.; JRMS, editors. Methods in Enzymology: Macromolecular Crystallography, part A. Vol. 276. Academic Press; 1997. p. 307-326.
30. McCoy AJ, et al. Phaser crystallographic software. J Appl Crystallogr. 2007; 40:658–674. [PubMed: 19461840]
31. Emsley P, Cowtan K. Coot: model-building tools for molecular graphics. Acta Crystallogr D Biol Crystallogr. 2004; 60:2126–32. [PubMed: 15572765]
32. Chen VB, et al. MolProbity: all-atom structure validation for macromolecular crystallography. Acta Crystallogr D Biol Crystallogr. 2010; 66:12–21. [PubMed: 20057044]

33. Laskowski RA, Rullmannn JA, MacArthur MW, Kaptein R, Thornton JM. AQUA and PROCHECK-NMR: programs for checking the quality of protein structures solved by NMR. J Biomol NMR. 1996; 8:477–86. [PubMed: 9008363]

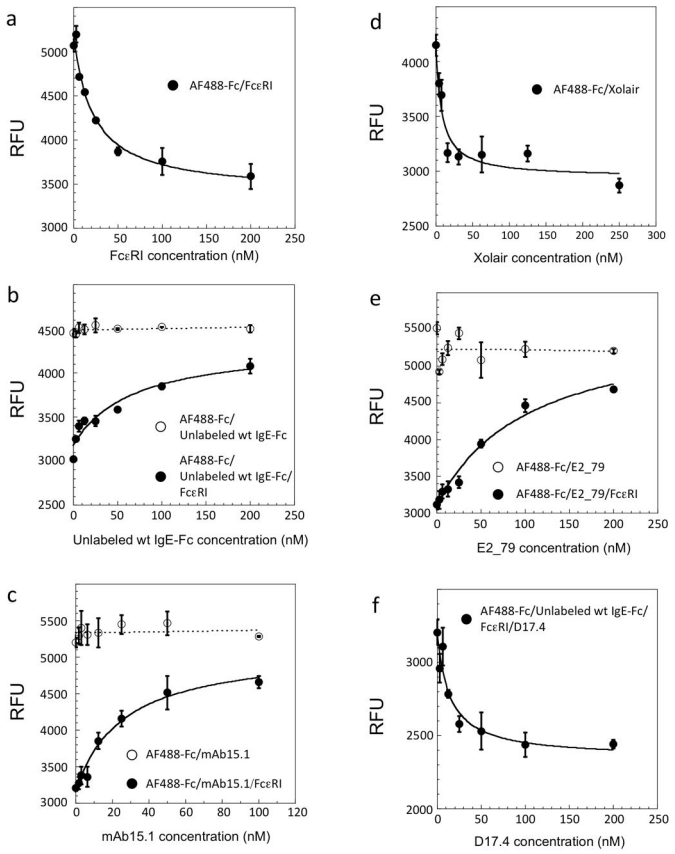

Figure 1. A fluorescence-quenching assay reveals different classes of IgE-directed inhibitors

(a) AF488-Fc fluorescence is quenched by FcεRIα. (b) Unlabelled IgE-Fc_{3-4} competes FcεRIα binding (filled circles, solid line), but has no effect on AF488-Fc alone (open circles, dotted line). (c) The anti-FcεRIα antibody mAb15.1 competes for FcεRIα binding (filled circles, solid line), but has no effect on AF488-Fc fluorescence (open circles, dotted line). (d) Omalizumab/Xolair quenches AF488-Fc fluorescence similar to FcεRIα. (e) E2_79 competes for FcεRIα binding (filled circles, solid line), but does not affect AF488-Fc fluorescence (open circles, dotted line). (f) D17.4 competes in assays containing AF488-Fc, FcεRIα and wt IgE-Fc_{3-4}, by binding IgE-Fc_{3-4} competitor (filled circles, solid line). Error bars represent standard deviations of replicate measurements.

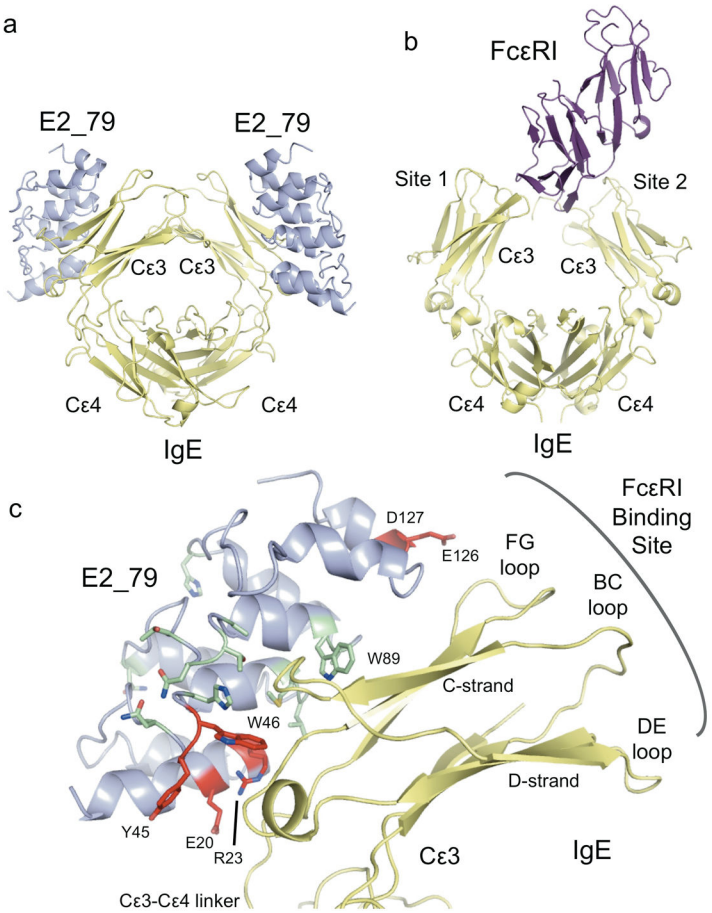

Figure 2. DARPin E2_79 binds IgE-Cε3 domains outside the FcεRIα binding site

(a) Crystal structure of the E2_79 (light blue) and C335 IgE-Fc_{3-4} (pale yellow) complex. (b) Structure of the IgE-Fc_{3-4}:FcεRIα complex oriented similarly to (a). FcεRIα (magenta) binds asymmetrically and two non-equivalent E2_79 binding sites (1 and 2) are indicated. (c) Residues in E2_79 at the interface with the IgE-Fc_{3-4} are shown as beige sticks. Mutated residues (E20, R23, Y45, W46, E126 and D127) are shown as red sticks. The FcεRIα binding loops (BC, DE and FG) in the Cε3 domain are indicated.

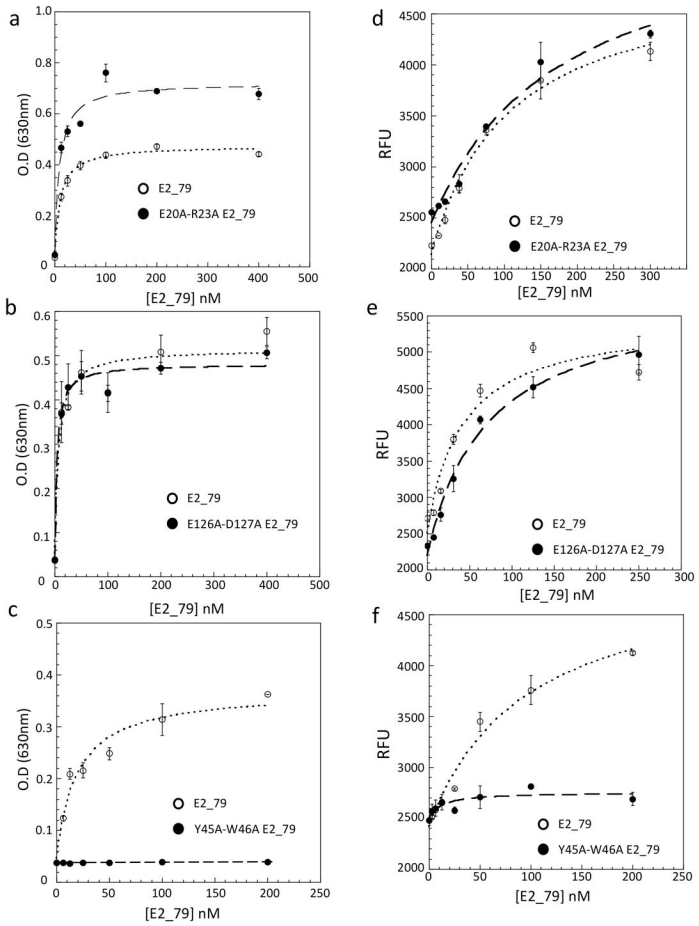

Figure 3. Binding and inhibition activities of E2_79 mutants

(a) The E20A-R23A mutant exhibits a binding affinity similar to wt E2_79. (b) The E126A-D127A mutant binds similarly to wt E2_79. (c) The Y45A-W46A mutant exhibits a loss of binding to IgE-Fc_{3-4}. (d) The E20A-R23A mutant inhibits FcεRIα binding similar to wt E2_79. (e) The E126A-D127A mutant inhibits FcεRIα binding similar to wt E2_79. (f) The Y45A-W46A mutant does not inhibit FcεRIα binding. Direct binding (a–c) was measured by ELISA. Inhibition was measured using the fluorescence quenching assay (d–f). Error bars represent standard deviations of replicate measurements.

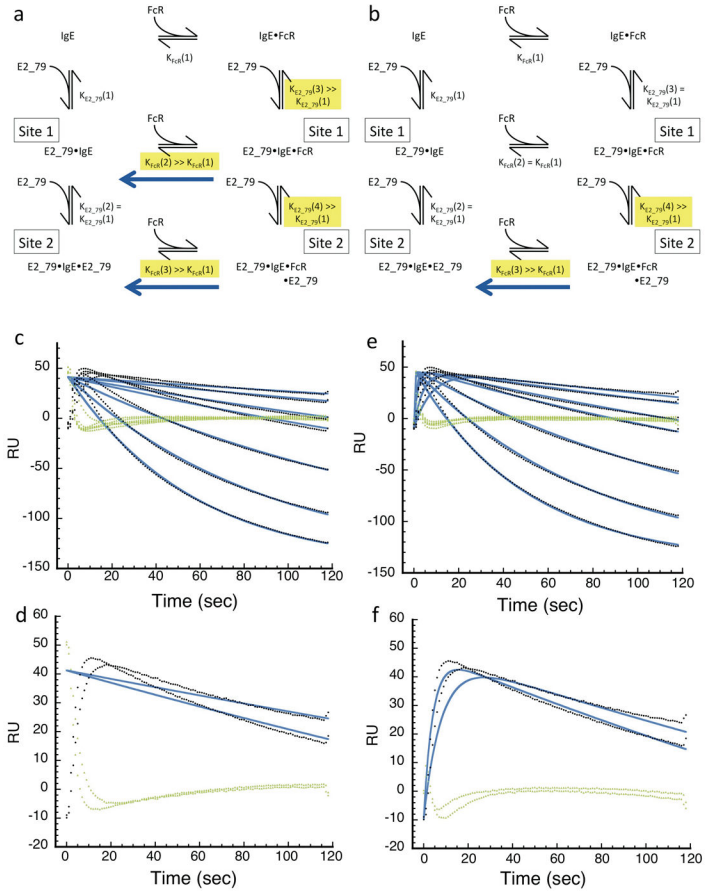

Figure 4. Kinetic modeling of SPR data points to a facilitated dissociation mechanism for E2_79

(a) Reaction scheme for the allosteric model. Blue arrows indicate IgE:FcεRIα complex dissociation is accelerated by E2_79 binding to Site 1 and Site 2. (b) Reaction scheme for the facilitated dissociation model. The blue arrow indicates that IgE:FcεRIα complex dissociation is only accelerated by E2_79 binding to Site 2. (c, d) Best global curve fitting result for the allosteric model, shown with seven concentrations of E2_79 (c), or the 100 nM and 200 nM E2_79 concentration curves (d). (e, f) Best global curve fitting result for the facilitated dissociation model, shown with seven concentrations of E2_79 (e), or the 100 nM and 200 nM E2_79 concentration curves (f). Rate and equilibrium dissociation constants highlighted in yellow were fit as described in methods. In panels c–f, black circles represent SPR data, fitted curves are colored blue and green triangles represent residual differences.